Published in final edited form as:
Biochemistry. 2009 August 25; 48(33): 8006–8013. doi:10.1021/bi901064k.

An Examination of the Relationship between Active Site Loop Size and Thermodynamic Activation Parameters for Orotidine 5′-Monophosphate Decarboxylase from Mesophilic and Thermophilic Organisms†

Krisztina Toth[§], **Tina L. Amyes**[§], **B. McKay Wood**[‡], **Kui K. Chan**[‡], **John A. Gerlt**[‡], and **John P. Richard**[§,*]

[§] Department of Chemistry, University at Buffalo, SUNY, Buffalo, New York 14260-3000

[‡] Departments of Biochemistry and Chemistry, University of Illinois, Urbana, Illinois 61801

Abstract

Closure of the active site phosphate gripper loop of orotidine 5′-monophosphate decarboxylase from *Saccharomyces cerevisiae* (ScOMPDC) over the bound substrate orotidine 5′-monophosphate (OMP) activates the bound substrate for decarboxylation by at least 10^4-fold [Amyes, T. L., Richard, J. P., and Tait, J. J. (2005) *J. Am. Chem. Soc. 127*, 15708-15709]. The 19 residue phosphate gripper loop of the mesophilic ScOMPDC is much larger than the 9 residue loop at the ortholog from the thermophile *Methanothermobacter thermautotrophicus* (MtOMPDC). This difference in loop size results in a small decrease in the total intrinsic phosphate binding energy of the phosphodianion group of OMP from 11.9 to 11.6 kcal/mol, along with a modest decrease in the extent of activation by phosphite dianion of decarboxylation of the truncated substrate 1-(β-D-erythrofuranosyl)orotic acid. The activation parameters $\Delta H^{\ddagger}$ and $\Delta S^{\ddagger}$ for k_{cat} for decarboxylation of OMP are 3.6 kcal/mol and 10 cal/K/mol more positive, respectively, for MtOMPDC than for ScOMPDC. We suggest that these differences are related to the difference in size of the active site loops at the mesophilic ScOMPDC and the thermophilic MtOMPDC. The greater enthalpic transition state stabilization available from the more extensive loop-substrate interactions for the ScOMPDC-catalyzed reaction is largely balanced by a larger entropic requirement for immobilization of the larger loop at this enzyme.

Orotidine 5′-monophosphate decarboxylase (OMPDC)[1] is a remarkable enzyme because it employs no metal ions or other cofactors but yet effects an enormous ca. 30 kcal/mol stabilization of the transition state for the chemically very difficult decarboxylation of orotidine 5′-monophosphate (OMP) to give uridine 5′-monophosphate (UMP) (Scheme 1) (1-3). The enormous 10^{17}-fold rate acceleration for decarboxylation of enzyme-bound OMP (k_{cat} = 15 s^{-1} (4)) is a consequence of the exceedingly slow decarboxylation of OMP in water ($t_{1/2} \approx 78$ million years (3)) through an unstable vinyl carbanion intermediate. This remarkable efficiency led to the proposal of several different mechanisms for the OMPDC-catalyzed reaction that

†This work was supported by Grants GM39754 to JPR and GM65155 to JAG from the National Institutes of Health.

* Author to whom correspondence should be addressed: Tel: (716) 645 4232, Fax: (716) 645 6963, jrichard@buffalo.edu.

[1]Abbreviations: OMP, orotidine 5′-monophosphate; UMP, uridine 5′-monophosphate; OMPDC, orotidine 5′-monophosphate decarboxylase; ScOMPDC, orotidine 5′-monophosphate decarboxylase from *Saccharomyces cerevisiae* (yeast); EcOMPDC, orotidine 5′-monophosphate decarboxylase from *Escherichia coli*; MtOMPDC, orotidine 5′-monophosphate decarboxylase from *Methanothermobacter thermautotrophicus*; EO, 1-(β-D-erythrofuranosyl)orotic acid; EU, 1-(β-D-erythrofuranosyl)uridine; DHAP, dihydroxyacetone phosphate; TIM, triosephosphate isomerase; GPDH, glycerol 3-phosphate dehydrogenase; MOPS, 3-(N-morpholino) propanesulfonic acid; IPTG, isopropyl β-D-thiogalactopyranoside; NADH, nicotinamide adenine dinucleotide, reduced form.

avoid formation of an unstable carbanion (5-10). However, we recently showed that OMPDC meets its catalytic challenge head-on by stabilizing an enzyme-bound vinyl carbanion (Scheme 1) (11,12).

One of the principal differences between catalysis by enzymes and by small molecules is that enzymes have evolved unique mechanisms to utilize binding interactions with nonreacting portions of the substrate for transition state stabilization (13). We have shown that the binding of phosphite dianion to OMPDC from *Saccharomyces cerevisiae* (yeast, ScOMPDC) results in an 80,000-fold increase in the second-order rate constant k_{cat}/K_m for enzyme-catalyzed decarboxylation of the truncated substrate 1-(β-D-erythrofuranosyl)orotic acid (EO), which lacks a 5′-phosphodianion moiety, to give 1-(β-D-erythrofuranosyl)uridine (EU) (Scheme 2) (14). This shows that the nonreacting phosphodianion group of OMP does not function simply to anchor the substrate to the enzyme, but rather serves the more important role of activating the enzyme towards decarboxylation of bound OMP.

Similar experiments provided evidence that the “intrinsic phosphate binding energy” of the substrate phosphodianion group of dihydroxyacetone phosphate (DHAP) is utilized in stabilization of the transition state of the aldose-ketose isomerization reaction catalyzed by triosephosphate isomerase (TIM) (15,16) and of the hydride transfer reaction catalyzed by glycerol 3-phosphate dehydrogenase (GPDH) (Scheme 3) (17).

OMPDC (10,18-22), TIM (23-25) and GPDH (26,27) each have a flexible “phosphate gripper” loop that is open at the free enzyme but closes over the phosphodianion group of bound substrate to sequester the substrate from bulk solvent. We have proposed that this phosphate-driven loop closure reduces the barrier for reaction at the loop-closed compared with the loop-open enzymes, and that it is the underlying origin of the $10^4 – 10^6$-fold effect of the nonreacting substrate phosphodianion group on the chemical reactivity of enzyme-bound substrate (17).

The phosphate gripper loops of ScOMPDC and of OMPDC from *Escherichia coli* (EcOMPDC) both extend 19 residues, from the strictly conserved Pro-202 to Val-220 for ScOMPDC (21) (Figure 1), and from Pro-189 to Pro-207 for EcOMPDC (19,20). By contrast, the corresponding loop of OMPDC from the thermophile *Methanothermobacter thermautotrophicus* (MtOMPDC) extends only 9 residues, from Pro-180 to Asp-188 (22) (Figure 1). These three enzymes show an otherwise high degree of structural homology (18) which then raises the question of whether there may be an underlying mechanistic imperative for the difference in the size of the flexible loops for enzymes from mesophiles and thermophiles. For example, if the size of this loop is related to catalytic efficiency, then the smaller loop for MtOMPDC might be expected to play a reduced role in promoting decarboxylation through utilization of the binding energy of the nonreacting substrate phosphodianion group of OMP or of a phosphite dianion activator.

We report here the results of experiments that were designed to compare the intrinsic phosphate binding energy and the thermodynamic activation parameters for OMPDCs from mesophilic and thermophilic organisms. The thermophilic enzyme with the shorter phosphate gripper loop, MtOMPDC, shows an intrinsic phosphate binding energy of the phosphodianion group of OMP and phosphite activation of decarboxylation of the truncated substrate EO that are similar to those observed for the mesophilic ScOMPDC. By contrast there is a significant difference in the activation parameters $\Delta H^{\ddagger}$ and $\Delta S^{\ddagger}$ for the decarboxylation of enzyme-bound OMP such that MtOMPDC pays a substantially smaller entropic price, but a larger enthalpic price, for conversion of the Michaelis complex to the transition state for decarboxylation than does ScOMPDC.

Experimental

Materials

Orotidine 5′-monophosphate trisodium salt (99%) was purchased from Sigma or was prepared by chemical or enzymatic methods from uridine 5′-monophosphate using modifications of literature procedures (28-30). 1-(β-D-Erythrofuranosyl)orotic acid (EO) and 1-(β-D-erythrofuranosyl)uridine (EU) were available from an earlier study (14). Sodium phosphite (dibasic, pentahydrate), 3-(N-morpholino)propanesulfonic acid (MOPS, ≥ 99.5%) and ammonium acetate (≥ 99%) were purchased from Fluka. Water was from a Milli-Q Academic purification system. All other chemicals were reagent grade or better and were used without further purification.

Preparation of OMPDCs

The C155S mutant OMPDC from *Saccharomyces cerevisiae* (ScOMPDC) was prepared as described previously (31,32). This mutant is more stable than, but kinetically and structurally essentially identical with, wildtype yeast OMPDC (33). Wildtype OMPDC from *Methanothermobacter thermautotrophicus* (MtOMPDC) was prepared as described previously (32). The gene for wildtype OMPDC from *Escherichia coli* (EcOMPDC) was cloned from *Escherichia coli* K12 genomic DNA by Dr. Wen Shan Yew and the protein was expressed in *E. coli* BL21 (DE3) using a modified pET-15b plasmid with a His_{10}-tag, as described previously for OMPDCs with a His_6-tag (32). The cells were grown at 37 °C, induced with IPTG (0.5 mM) when the cell density reached an OD_{600} of 0.6, and harvested after 18 h. Purification was carried out as described previously for ScOMPDC and MtOMPDC (32) except that no Q-Sepharose column was used. The protein was dialyzed at 5 °C against the storage buffer (20 mM Tris-HCl, pH 7.0, 100 mM NaCl and 20% glycerol), concentrated to ca. 25 mg/mL via ultrafiltration, flash frozen in liquid nitrogen as 25 μL pellets and stored at -80 °C.

Preparation of Solutions

Solution pH was determined at 25 °C using an Orion Model 720A pH meter equipped with a Radiometer pHC4006-9 combination electrode that was standardized at pH 7.00 and 10.00 at 25 °C. Stock solutions of OMP were prepared in water and the OMP concentration was determined from the absorbance in 0.1 M HCl at 267 nm using $\varepsilon = 9430\ M^{-1}\ cm^{-1}$ (34). Stock solutions of 1-(β-D-erythrofuranosyl)orotic acid (EO) were prepared and neutralized to pH ≈ 6 as described in earlier work (14,31) and the EO concentration was determined from the absorbance in 0.1 M HCl at 267 nm using $\varepsilon = 9570\ M^{-1}\ cm^{-1}$ reported for orotidine (34).

The stock solution of phosphite (100 mM, 80% free base, $I = 0.28$) was prepared by addition of a measured amount of 1 M HCl to the sodium salt to give the desired acid/base ratio. MOPS buffers were prepared by addition of measured amounts of 1 M HCl and solid NaCl to give the desired acid/base ratio and ionic strength.

Samples of OMPDCs that had been stored at -80 °C were defrosted and dialyzed at 4 °C against 10 mM MOPS (50% free base) at pH 7.1 containing 100 mM NaCl, unless noted otherwise.

Determination of Values of k_{cat} and k_{cat}/K_m for Turnover of OMP by OMPDCs at Various Temperatures

All assays were carried out in 10 mM MOPS (50% free base) at pH 7.1 and $I = 0.105$ (NaCl) using a Cary 3E spectrophotometer equipped with a temperature-controlled Peltier block multicell changer. The temperature dependence of the difference between the extinction coefficients of OMP and UMP at 279 nm, $\Delta\varepsilon$ ($M^{-1}\ cm^{-1}$), was determined using the following procedure: First the spectrophotometer was zeroed at 279 nm using a solution of 10 mM MOPS at pH 7.1 and $I = 0.105$ (NaCl) at 25 °C. A small aliquot of OMP was added to give a final

concentration of 100 μM OMP and the absorbance of the resulting solution was determined at several temperatures between 10 and 75 °C. The temperature was then returned to 25 °C and 1 μL of a solution of ScOMPDC was added to give a final enzyme concentration of 21 nM. The ensuing decarboxylation of OMP was allowed to proceed to completion to give a quantitative yield of UMP and the final absorbance of the solution was again determined at several temperatures between 10 and 75 °C. The observed absorbance changes were used to calculate the following values of $\Delta\varepsilon$ (M^{-1} cm^{-1}): 10 °C, 2290; 25 °C, 2400 (4); 35 °C, 2490; 45 °C, 2560; 55 °C, 2610; 65 °C, 2660; 75 °C, 2720. The following values of $\Delta\varepsilon$ at other temperatures were obtained by extrapolation or interpolation using the two linear regions of the biphasic linear correlation between $\Delta\varepsilon$ (M^{-1} cm^{-1}) and T (°C): 5 °C, 2250; 12 °C, 2300; 15 °C, 2330; 17 °C, 2340.

For the determination of values of k_{cat} the reaction mixtures (1 mL total) containing buffer and OMP ($[OMP]_o$ = 50 - 250 μM, $\gg 10K_m$] were equilibrated at the temperature of interest and the reaction was initiated by the addition of 1 - 3 μL of a stock solution of OMPDC using a cuvette admixer without removal of the cuvette from the temperature-controlled block. The initial velocity of decarboxylation of OMP under these conditions, V_{max} (M s^{-1}), was determined within 1 min by monitoring the decrease in absorbance at 279 nm using the appropriate value of $\Delta\varepsilon$ (M^{-1} cm^{-1}) for the temperature of interest. The observed values of V_{max} were generally shown to be proportional to enzyme concentration in the following ranges: ScOMPDC, 11 - 42 nM; MtOMPDC, 76 - 150 nM; EcOMPDC, 30 - 230 nM. At some temperatures the use of lower concentrations of OMPDC resulted in reduced activity, presumably as a result of dissociation of the active dimer to give the inactive monomeric form (4). These conditions were: 38 nM MtOMPDC at 45 or 55 °C, k_{cat} was reduced by 20%; 30 nM EcOMPDC at 10 °C, k_{cat} was reduced by 30% (the data were therefore obtained using 60 nM enzyme); 30 nM EcOMPDC at 5 °C, k_{cat} was reduced by 50% (the data were therefore obtained using 90 – 230 nM enzyme); 15 nM EcOMPDC at 25 °C, k_{cat} was reduced by 20%. In order to verify that the temperature variation did not result in a loss of enzyme activity in the timeframe of the assays which were conducted over a period of ≤ 1 min (see above), periodic controls were conducted in which the stock solution of OMPDC was incubated in a water bath at the assay temperature of interest for 1 – 5 min prior to its use in the assay at this temperature. It was found that this preincubation did not significantly affect the observed activity at the temperature of interest.

Values of k_{cat} (s^{-1}) were calculated from the values of V_{max} (M s^{-1}) using eq 1. In all cases the concentration of ScOMPDC in the stock solution was calculated from the values of V_{max} (M s^{-1}) determined in side-by-side standard assays at 25 °C using eq 1 with k_{cat} = 15 s^{-1} (4). For determination of the values of k_{cat} at 25 °C for MtOMPDC (4.7 s^{-1}) and EcOMPDC (13 s^{-1}) the concentration of OMPDC was determined from the absorbance of the protein at 280 nm in 10 mM MOPS (50% free base) at pH 7.1 containing 100 mM NaCl and the extinction coefficients of 6100 M^{-1} cm^{-1} (MtOMPDC) and 10100 M^{-1} cm^{-1} (EcOMPDC) that were calculated using the ProtParam tool available on the ExPASy server (35,36). For determination of the values of k_{cat} at other temperatures the concentrations of MtOMPDC and EcOMPDC were determined from the values of V_{max} (M s^{-1}) determined in side-by-side standard assays at 25 °C using eq 1 with k_{cat} = 4.7 s^{-1} and 13 s^{-1}, respectively.

$$k_{cat} = V_{max}/[E] \quad (1)$$

Values of k_{cat}/K_m for turnover of OMP by ScOMPDC and MtOMPDC at various temperatures were determined in experiments in which the complete disappearance of a relatively low initial concentration OMP was monitored at 279 nm. Reactions (1 mL total, $[OMP]_o$ = 4 – 40 μM)

were initiated by the addition of OMPDC as described above to give a final concentration of 20 – 70 nM ScOMPDC or 50 – 420 nM MtOMPDC. The observed rate constants k_{obsd} (s^{-1}) for the first-order decay of OMP in the final stages of the reactions where $[OMP]_t \leq 0.3 – 0.5K_m$ were obtained from the fits of the absorbance vs time data to a single exponential. Experiments were conducted at several enzyme concentrations in the indicated ranges to ensure that the observed first-order decay represents enzyme-catalyzed reaction of OMP rather than a loss of enzyme activity with time, and the values of k_{obsd} were shown to be proportional to [E]. Values of k_{cat}/K_m (M^{-1} s^{-1}) were then calculated using the relationship $k_{cat}/K_m = k_{obsd}/[E]$ and values of K_m for OMP were obtained by combining the experimental values of k_{cat} (s^{-1}) and k_{cat}/K_m (M^{-1} s^{-1}) (see Table 1). In all cases the concentration of OMPDC was determined from the values of V_{max} (M s^{-1}) determined in side-by-side standard assays at 25 °C using eq 1 with the appropriate value of k_{cat}. This analysis is possible because the *initial* concentration of OMP in these experiments ($[OMP]_o \leq 40$ μM) was chosen (see below) such that the amount of the UMP product generated (≤ 40 μM) is insufficient to result in significant inhibition of the OMPDC of interest. The initial concentration of OMP ($[OMP]_o$) was chosen based on the following: For ScOMPDC a value of K_i = 400 μM has been reported for binding of UMP to ScOMPDC at 25 °C under our experimental conditions (4), and there was no significant change in the value of K_m determined in our experiments at 45 °C for $[OMP]_o$ = 11 – 33 μM. For MtOMPDC at 25 °C experiments conducted at $[OMP]_o$ = 200 – 400 μM yielded *apparent* values of K_m that are consistent with values of K_i for binding of UMP to MtOMPDC of ca. 100 μM at 25 °C and ca. 200 μM at 55 °C. There was no significant change in the value of K_m determined in our experiments when the initial concentration of OMP was varied in the range 6 – 30 μM at 5 °C, 4 – 12 μM at 25 °C, 12 – 22 μM at 35 °C, or 18 – 39 μM at 55 °C.

Turnover of EO by MtOMPDC in the Absence and Presence of Phosphite Dianion

The decarboxylation of the truncated substrate 1-(β-D-erythrofuranosyl)orotic acid (EO, 5 mM) in 50 mM MOPS (45% free base) at pH 7.0, 25 °C and I = 0.14 (NaCl) catalyzed by MtOMPDC (350 μM) was followed in a discontinuous assay in which the initial velocity of formation of the product 1-(β-D-erythrofuranosyl)uridine (EU) was monitored by HPLC. For these experiments MtOMPDC was dialyzed at 4 °C against 100 mM MOPS (45% free base) at pH 7.0 and I = 0.28 (NaCl). The reaction in a total volume of 200 μL was initiated by the addition of EO to a solution of the enzyme in buffer that was equilibrated at 25 °C. The reaction was followed for ca. 7 h, during which time there was 8% reaction of EO. At various times an aliquot (20 μL) was withdrawn and quenched to pH 3.8 by the addition of 180 μL of ice-cold 5 mM formic acid. The enzyme was removed by ultrafiltration using an Amicon Microcon filtration device (10K MWCO) and the filtrate (150 μL) was analyzed by HPLC using a using a Waters Atlantis dC_{18} 3 μm column (3.9 × 150 mm) with an isocratic flow of 1 mL/min 10 mM NH_4OAc (pH 4.2) and peak detection at 262 nm. Under these conditions the unreacted EO eluted close to the void volume and the product EU eluted at ca. 7 min. The concentration of the product EU in the reaction mixture at time t, $[EU]_t$, was obtained from the HPLC peak area by interpolation of a standard curve that was constructed using authentic EU. The concentration of MtOMPDC in the reaction mixture was determined by periodic standard assay (see above) and it was shown that there was no significant decrease in enzyme activity during the reaction. The initial velocity of the reaction, v_i (M s^{-1}), was determined as the slope of the linear plot of $[EU]_t$ against time. The second-order rate constant $(k_{cat}/K_m)_o$ (M^{-1} s^{-1}) for MtOMPDC-catalyzed decarboxylation of EO was calculated using the relationship $(k_{cat}/K_m)_o = v_i/[E]\,[S]_o$.

The decarboxylation of EO (0.12 mM) in the presence of 2 – 36 mM phosphite dianion and 5 mM MOPS at pH 7.0, 25 °C and I = 0.14 (NaCl) catalyzed by MtOMPDC (22 – 38 μM) was monitored spectrophotometrically at 283 nm. Reactions (1 mL total) were initiated by the addition of 50 μL of a solution of MtOMPDC in 100 mM MOPS (pH 7.0, I = 0.28, NaCl) and

were monitored for up to 6 h. The concentration of MtOMPDC in the reaction mixture was determined by standard assay and it was shown that there was no significant decrease in enzyme activity during the reaction. These reactions obeyed excellent first-order kinetics with stable endpoints and values of k_{obsd} (s^{-1}) for the reaction of EO were obtained from the fits of the absorbance vs time data to a single exponential. The apparent second-order rate constants $(k_{cat}/K_m)_{obsd}$ (M^{-1} s^{-1}) for MtOMPDC-catalyzed decarboxylation of EO at the various concentrations of phosphite dianion were calculated using the relationship $(k_{cat}/K_m)_{obsd} = k_{obsd}/[E]$.

Results

The second-order rate constant for decarboxylation of the truncated substrate 1-(β-D-erythrofuranosyl)orotic acid (EO) lacking a 5′-phosphodianion group catalyzed by OMPDC from *Methanothermobacter thermautotrophicus* (MtOMPDC) at pH 7.0, 25 °C and I = 0.14 (NaCl) was determined as $(k_{cat}/K_m)_o = 8.7 \times 10^{-3}$ M^{-1} s^{-1} (Table 1).

Figure 2 shows the dependence of the apparent second-order rate constant $(k_{cat}/K_m)_{obsd}$ (Table 1) for decarboxylation of the truncated substrate EO catalyzed by MtOMPDC on the concentration of added phosphite dianion at pH 7.0, 25 °C and I = 0.14 (NaCl). There is no evidence for saturation of MtOMPDC by phosphite dianion and the data for $[HPO_3^{2-}] < 30$ mM show a good fit to eq 2 that was derived for the mechanism shown in Scheme 4 with $[HPO_3^{2-}] \ll K_d$. The slope of the correlation gives the third-order rate constant for the phosphite-activated reaction as $(k_{cat}/K_m)_{E\cdot HPi}/K_d = 2500$ M^{-2} s^{-1} (Table 1). However, there are small (ca. 30%) positive deviations of the data at $[HPO_3^{2-}] = 36$ mM from the linear correlation established for $[HPO_3^{2-}] < 30$ mM (Figure 2). A control experiment at $[HPO_3^{2-}] = 18$ mM, $[Cl^-] = 12$ mM and $[NO_3^-] = 63$ mM (I = 0.14) gave a value of $(k_{cat}/K_m)_{obsd} = 6.3$ M^{-1} s^{-1}, which is 7-fold lower than the corresponding value of 46 M^{-1} s^{-1} determined at $[HPO_3^{2-}] = 18$ mM and $[Cl^-] = 75$ mM (I = 0.14). This suggests that there are specific salt effects on the activity of MtOMPDC associated with the replacement of chloride with other anions.

$$(k_{cat}/K_m)_{obsd} = (k_{cat}/K_m)_o + \frac{(k_{cat}/K_m)_{E\cdot HPi}[HPO_3^{2-}]}{K_d} \quad (2)$$

Table 2 reports the kinetic parameters k_{cat}, k_{cat}/K_m and K_m for decarboxylation of OMP catalyzed by ScOMPDC, MtOMPDC and EcOMPDC at various temperatures between 5 °C and 55 °C. Care was taken to work at concentrations of OMPDC where the enzyme exists mainly in the active dimeric form (4). It was routinely shown that the kinetic parameters are independent of the concentration of both OMPDC and the initial concentration of OMP used for their determination. Control experiments were conducted to ensure that there that the temperature variation did not result in a loss of enzyme activity in the timeframe of the assays.

Discussion

A comparison of the kinetic parameters for decarboxylation of the whole substrate OMP and the truncated substrate EO (Table 1) shows that the binding interactions between the enzyme and the 5′-phosphodianion group of OMP are responsible for the 5.2×10^8 and 3.6×10^8-fold increases, respectively, in the second-order rate constant for decarboxylation of the truncated substrate EO catalyzed by ScOMPDC and MtOMPDC. These rate increases correspond to similar intrinsic phosphate binding energies of 11.9 and 11.6 kcal/mol, respectively (14). These results are consistent with a somewhat larger transition state stabilization from interactions of the phosphodianion group of the enzyme-bound ligand with the long flexible phosphate gripper

loop of the mesophilic ScOMPDC (19 residues) compared with the shorter flexible loop of the thermophilic MtOMPDC (9 residues) (Figure 1).

We have reported intrinsic phosphate binding energies of 12.2 and ≥ 11.0 kcal/mol for the deprotonation of *R*-glyceraldehyde 3-phosphate catalyzed by TIM (16) and the reduction of DHAP by NADH catalyzed by GPDH (17), respectively, each of which has a phosphate gripper loop that results in optimal interaction of the substrate phosphodianion group with the protein catalyst (23-27). The similarity in the intrinsic phosphate binding energies for three enzymes that catalyze a variety of chemical reactions suggests that 12 kcal/mol serves as the effective upper limit on the intrinsic phosphate binding energy obtained after billions of years of evolutionary pressure to select for optimal protein catalysts of these different reactions. We suggest that phosphate gripper loops are essential to obtaining this large intrinsic phosphate binding energy, because they provide the protein with the means to make a maximal number of contacts with the substrate, which binds initially at an open active site cleft and then becomes buried in the protein interior upon loop closure (13,37).

We reported earlier that the binding of phosphite dianion to ScOMPDC strongly activates the enzyme toward decarboxylation of the truncated substrate EO lacking a 5′-phosphodianion group (14). Figure 2 shows that phosphite dianion is also a potent activator of the decarboxylation of EO catalyzed by MtOMPDC. The ratio of the third-order rate constant $(k_{cat}/K_m)_{E\cdot HPi}/K_d$ (Scheme 4) for the phosphite-activated decarboxylation of EO and the second-order rate constant $(k_{cat}/K_m)_o$ for the unactivated decarboxylation of EO provides a good measure of the extent of activation by sub-saturating concentrations of phosphite dianion. The values of the ratios of $\{(k_{cat}/K_m)_{E\cdot HPi}/K_d\}/(k_{cat}/K_m)_o = 5.6 \times 10^5\ M^{-1}$ and $2.9 \times 10^5\ M^{-1}$ for the reactions catalyzed by ScOMPDC and MtOMPDC (Table 1) shows that the larger flexible phosphate gripper loop at the enzyme from yeast results in slightly larger advantage from phosphite activation. We conclude that the large reduction in loop size for the thermophilic compared with mesophilic enzyme does not have a severe effect on either phophodianion activation of the whole OMP, or phosphite dianion activation of the truncated substrate EO.

Temperature Dependence of k_{cat} for OMPDCs from Various Organisms

Figure 3 shows Eyring plots of k_{cat} for decarboxylation of OMP catalyzed by ScOMPDC, MtOMPDC and EcOMPDC over the temperature range 5 – 55 °C (278 – 328 K) according to eq 3. Table 3 gives the derived values of $\Delta H^{\ddagger}$ and $\Delta S^{\ddagger}$ that were calculated from the slopes ($-\Delta H^{\ddagger}/R$) and intercepts ($\Delta S^{\ddagger}/R$) of these correlations, respectively. The activation parameters for ScOMPDC and EcOMPDC are very similar so that there is almost no change in the relative values of k_{cat} for these enzymes with changing temperature. However, the ratio of the values of k_{cat} for ScOMPDC and MtOMPDC decreases from 4.8 at 5 °C to 1.9 at 45 °C, which reflects the larger value of $\Delta H^{\ddagger}$ for MtOMPDC (14.8 kcal/mol, Table 3) than for ScOMPDC (11.2 kcal/mol). These results show that, compared with ScOMPDC, MtOMPDC makes better use of the greater thermal energy that is available at the higher temperature maximum for this thermophilic enzyme.

$$\ln\left(k_{cat}h/k_{B}T\right) = \frac{\Delta S^{\ddagger}}{R} - \frac{\Delta H^{\ddagger}}{RT} \quad (3)$$

The entropy of activation for MtOMPDC (-6.0 cal K^{-1} mol^{-1}, Table 3) is more positive than for ScOMPDC (-16 cal K^{-1} mol^{-1}), so that there is a *larger* unfavorable enthalpic and *smaller* unfavorable entropic change for conversion of the ground state Michaelis complex to the transition state for MtOMPDC-catalyzed decarboxylation than for the ScOMPDC-

catalyzed reaction. We suggest that the difference in the size of the active site loops at MtOMPDC and ScOMPDC results in the observed difference in the activation parameters for these enzymes. The greater enthalpic transition state stabilization may reflect the more extensive loop-substrate interactions for the ScOMPDC-catalyzed reaction, and these are suggested to be balanced by a greater entropic requirement for immobilization of the larger loop at the ES complex and transition state for the yeast enzyme. A similar difference in the enthalpy and entropy of activation has been observed for the mesophilic lactate dehydrogenase from *Deinococcus radiourans* and the corresponding thermophilic enzyme from *Thermus thermophilus* where the role of loops in catalysis is less well defined (13).

For many enzymes it has been shown that increases in protein thermostability are often the result of enhanced networks of stabilizing ionic interactions between the side chains of amino acid residues (38). These added ionic interactions have the effect of restricting protein conformational changes, so that, at the same temperature, enzymes from thermophiles are often more rigid than their mesophilic counterparts (39,40). For example, a study of neutron scattering by the thermophilic malate dehydrogenase from *Methanococcus jannachii* and a mesophilic analog, lactate dehydrogenase from *Orytolagus cunniliculus* (rabbit muscle), shows that the root mean square fluctuations (1.5 Å) are similar for these enzymes at the temperature of their optimal activity (41). The similar conformational flexibility observed for enzymes at their temperature optimum suggests that the restriction of protein motions below a threshold level might cripple catalytic activity (40,42,43). Similarly, loop movement is required both to trap OMPDC-bound substrate (loop closure) and to release the product (loop opening), but yet the loop must remain fixed as the loop-closed enzyme-substrate complex is converted to product.

We suggest that efficient substrate binding and catalysis requires both flexibility of the loop to allow for efficient transport of the ligand to and from OMPDC, but also rigidity at the closed ES and $ES^{\ddagger}$ complexes. Truncation of the large flexible phosphate gripper loop for the mesophilic enzyme on moving to the thermophilic MtOMPDC might maintain this balance by reducing high-temperature motion of the loop when it is closed over the substrate. This would have the additional effect of reducing the stabilizing interactions between the loop and the substrate phosphodianion group, thereby leading to an increase in $\Delta H^{\ddagger}$ and a decrease in the kinetic parameters for the reaction catalyzed by the thermophilic enzyme at 25 °C (Figure 3). However, the increase in $\Delta H^{\ddagger}$ also sharpens the temperature dependence for the thermophilic enzyme-catalyzed reaction and helps to ensure that the thermophilic and mesophilic enzymes have similar kinetic parameters at their respective operating temperatures.

Temperature Effects on k_{cat}/K_m for OMPDCs from Various Organisms

Figure 4 shows the effect of changing temperature on k_{cat}/K_m for decarboxylation of OMP catalyzed by ScOMPDC and MtOMPDC. For both enzymes roughly linear correlations of ln (k_{cat}/K_m) with 1/T are observed at low temperature (< 35 °C, 308 K) where the value of K_m is essentially constant and the overall change in k_{cat}/K_m is due to the increase in k_{cat} with increasing T (Table 2). For ScOMPDC there is a sharp downward break in the correlation at 35 °C (308 K) where $k_{cat}/K_m = 1.7 \times 10^7\ M^{-1}\ s^{-1}$ reaches a maximum (Table 2). This downward break reflects the sharp increases in the Michaelis constant K_m with increasing temperature, which outweigh the increases in k_{cat}. These observations are consistent with a change in rate-determining step for k_{cat}/K_m for ScOMPDC from rate-determining decarboxylation (k_{cat}, $k_{-1} > k_{cat}$, eq 4) for reactions at low temperature, to rate-determining substrate binding (k_1, $k_{-1} < k_{cat}$, eq 4) for reactions at higher temperatures (Scheme 5) (44,45). The fractional dependence of k_{cat}/K_m on solvent viscosity (32) and the experimental rate constant ratio (k_{-1}/k_{cat}) ≈ 4 (4) determined for ScOMPDC-catalyzed decarboxylation of OMP at 25 °C both show that substrate binding (k_1) is already partly rate-determining at this temperature. Therefore, if the

temperature dependence of k_{-1} for breakdown of the E·OMP complex is small, a change in rate-determining step with increasing temperature should be observed (Scheme 5).

$$k_{cat}/K_m = \left(\frac{k_1 k_{cat}}{k_{-1}+k_{cat}}\right) \quad (4)$$

For MtOMPDC the downward break in the correlation in Figure 4 at 25 °C (298 K) where $k_{cat}/K_m = 3.1 \times 10^6\ M^{-1}\ s^{-1}$ is probably due to a similar change in rate-determining step for the reaction of OMP. The difference in the limiting values of $k_{cat}/K_m = 6.1 \times 10^6\ M^{-1}\ s^{-1}$ (T = 55 °C, Table 2) and $1.7 \times 10^7\ M^{-1}\ s^{-1}$ (T = 25 °C, Table 2) for the reactions catalyzed by MtOMPDC and ScOMPDC, respectively, suggests that simple diffusion of substrate to the enzyme active sites cannot be rate determining for both reactions. We suggest that the barrier to loop-reorganization to "trap" the substrate at the enzyme active site contributes to the activation barriers for encounter-complex formation, and that this former barrier is larger for the MtOMPDC-catalyzed reaction.

Conclusions and Speculation

A large positive $\Delta H^{\ddagger}$ allows thermophilic enzymes to make efficient use of the large thermal heat energy available from their environment by maximizing the increase in reactivity as the temperature is increased. A small negative $\Delta S^{\ddagger}$ will minimize unfavorable temperature effects associated with an increase in "order" on proceeding from the enzyme-substrate complex to the transition state. We suggest that these thermodynamic constraints favor the evolution of truncated flexible active site loops at enzymes from thermophilic organisms. The results reported here support the conclusion that the relatively short flexible phosphate gripper loop at OMPDC from the thermophile *M. thermautotrophicus* provides a smaller enthalpic transition state stabilization, but that this enthalpic stabilization carries a lower entropic price, compared with the transition state stabilization provided by the larger loops at OMPDCs from the mesophiles *S. cerevisiae* and *E. coli*. This tentative conclusion is not meant to minimize the possible relevance and contribution of other protein motions to the activation barriers for enzyme-catalyzed reactions.

References

1. Callahan BP, Miller BG. OMP decarboxylase - An enigma persists. Bioorg Chem 2007;35:465–469. [PubMed: 17889251]
2. Miller BG, Wolfenden R. Catalytic proficiency: the unusual case of OMP decarboxylase. Annu Rev Biochem 2002;71:847–885. [PubMed: 12045113]
3. Radzicka A, Wolfenden R. A proficient enzyme. Science 1995;267:90–93. [PubMed: 7809611]
4. Porter DJT, Short SA. Yeast Orotidine-5′-Phosphate Decarboxylase: Steady-State and Pre-Steady-State Analysis of the Kinetic Mechanism of Substrate Decarboxylation. Biochemistry 2000;39:11788–11800. [PubMed: 10995247]
5. Stanton CL, Kuo IF, Mundy CJ, Laino T, Houk KN. QM/MM metadynamics study of the direct decarboxylation mechanism for orotidine-5′-monophosphate decarboxylase using two different QM regions: acceleration too small to explain rate of enzyme catalysis. J Phys Chem B 2007;111:12573–12581. [PubMed: 17927240]
6. Silverman R, Groziak M. Model chemistry for a covalent mechanism of action of orotidine 5′-phosphate decarboxylase. J Am Chem Soc 1982;104:6434–6439.
7. Shostak K, Jones ME. Orotidylate decarboxylase: insights into the catalytic mechanism from substrate specificity studies. Biochemistry 1992;31:12155–12161. [PubMed: 1457411]
8. Lee JK, Houk KN. A proficient enzyme revisited: the predicted mechanism for orotidine monophosphate decarboxylase. Science 1997;276:942–945. [PubMed: 9139656]

9. Lee TS, Chong LT, Chodera JD, Kollman PA. An alternative explanation for the catalytic proficiency of orotidine 5′-phosphate decarboxylase. J Am Chem Soc 2001;123:12837–12848. [PubMed: 11749542]
10. Appleby TC, Kinsland C, Begley TP, Ealick SE. The crystal structure and mechanism of orotidine 5′-monophosphate decarboxylase. Proc Natl Acad Sci U S A 2000;97:2005–2010. [PubMed: 10681442]
11. Toth K, Amyes TL, Wood BM, Chan K, Gerlt JA, Richard JP. Product Deuterium Isotope Effect for Orotidine 5′-Monophosphate Decarboxylase: Evidence for the Existence of a Short-Lived Carbanion Intermediate. J Am Chem Soc 2007;129:12946–12947. [PubMed: 17918849]
12. Amyes TL, Wood BM, Chan K, Gerlt JA, Richard JP. Formation and Stability of a Vinyl Carbanion at the Active Site of Orotidine 5′-Monophosphate Decarboxylase: pK_a of the C-6 Proton of Enzyme-Bound UMP. J Am Chem Soc 2008;130:1574–1575. [PubMed: 18186641]
13. Jencks WP. Binding energy, specificity, and enzymic catalysis: the Circe effect. Adv Enzymol Relat Areas Mol Biol 1975;43:219–410. [PubMed: 892]
14. Amyes TL, Richard JP, Tait JJ. Activation of orotidine 5′-monophosphate decarboxylase by phosphite dianion: The whole substrate is the sum of two parts. J Am Chem Soc 2005;127:15708–15709. [PubMed: 16277505]
15. Amyes TL, Richard JP. Enzymatic catalysis of proton transfer at carbon: activation of triosephosphate isomerase by phosphite dianion. Biochemistry 2007;46:5841–5854. [PubMed: 17444661]
16. Amyes TL, O'Donoghue AC, Richard JP. Contribution of phosphate intrinsic binding energy to the enzymatic rate acceleration for triosephosphate isomerase. J Am Chem Soc 2001;123:11325–11326. [PubMed: 11697989]
17. Tsang WY, Amyes TL, Richard JP. A Substrate in Pieces: Allosteric Activation of Glycerol 3-Phosphate Dehydrogenase (NAD+) by Phosphite Dianion. Biochemistry 2008;47:4575–4582. [PubMed: 18376850]
18. Begley TP, Ealick SE. Enzymatic reactions involving novel mechanisms of carbanion stabilization. Curr Opin Chem Biol 2004;8:508–515. [PubMed: 15450493]
19. Harris P, Poulsen JCN, Jensen KF, Larsen S. Structural basis for the catalytic mechanism of a proficient enzyme: orotidine 5′-monophosphate decarboxylase. Biochemistry 2000;39:4217–4224. [PubMed: 10757968]
20. Harris P, Poulsen JC, Jensen KF, Larsen S. Substrate binding induces domain movements in orotidine 5′-monophosphate decarboxylase. J Mol Biol 2002;318:1019–1029. [PubMed: 12054799]
21. Miller BG, Hassell AM, Wolfenden R, Milburn MV, Short SA. Anatomy of a proficient enzyme: the structure of orotidine 5′-monophosphate decarboxylase in the presence and absence of a potential transition state analog. Proc Natl Acad Sci U S A 2000;97:2011–2016. [PubMed: 10681417]
22. Wu N, Mo Y, Gao J, Pai EF. Electrostatic stress in catalysis: structure and mechanism of the enzyme orotidine monophosphate decarboxylase. Proc Natl Acad Sci U S A 2000;97:2017–2022. [PubMed: 10681441]
23. Sampson NS, Knowles JR. Segmental movement: definition of the structural requirements for loop closure in catalysis by triosephosphate isomerase. Biochemistry 1992;31:8482–8487. [PubMed: 1390632]
24. Sampson NS, Knowles JR. Segmental motion in catalysis: investigation of a hydrogen bond critical for loop closure in the reaction of triosephosphate isomerase. Biochemistry 1992;31:8488–8494. [PubMed: 1390633]
25. Pompliano DL, Peyman A, Knowles JR. Stabilization of a reaction intermediate as a catalytic device: definition of the functional role of the flexible loop in triosephosphate isomerase. Biochemistry 1990;29:3186–3194. [PubMed: 2185832]
26. Ou X, Ji C, Han X, Zhao X, Li X, Mao Y, Wong LL, Bartlam M, Rao Z. Crystal structures of human glycerol 3-phosphate dehydrogenase 1 (GPD1). J Mol Biol 2006;357:858–869. [PubMed: 16460752]
27. Suresh S, Turley S, Opperdoes FR, Michels PAM, Hol WGH. A potential target enzyme for trypanocidal drugs revealed by the crystal structure of NAD-dependent glycerol-3-phosphate dehydrogenase from *Leishmania mexicana*. Structure 2000;8:541–552. [PubMed: 10801498]

28. Smiley JA, Paneth P, O'Leary MH, Bell JB, Jones ME. Investigation of the enzymic mechanism of yeast orotidine-5′-monophosphate decarboxylase using carbon-13 kinetic isotope effects. Biochemistry 1991;30:6216–6223. [PubMed: 2059628]
29. Miller BG, Butterfoss GL, Short SA, Wolfenden R. Role of Enzyme-Ribofuranosyl Contacts in the Ground State and Transition State for Orotidine 5′-Phosphate Decarboxylase: A Role for Substrate Destabilization? Biochemistry 2001;40:6227–6232. [PubMed: 11371183]
30. Van Vleet JL, Reinhardt LA, Miller BG, Sievers A, Cleland WW. Carbon isotope effect study on orotidine 5′-monophosphate decarboxylase: support for an anionic intermediate. Biochemistry 2008;47:798–803. [PubMed: 18081312]
31. Barnett SA, Amyes TL, Wood BM, Gerlt JA, Richard JP. Dissecting the Total Transition State Stabilization Provided by Amino Acid Side Chains at Orotidine 5′-Monophosphate Decarboxylase: A Two-Part Substrate Approach. Biochemistry 2008;47:7785–7787. [PubMed: 18598058]
32. Wood BM, Chan KK, Amyes TL, Richard JP, Gerlt JA. Mechanism of the Orotidine 5′-Monophosphate Decarboxylase-Catalyzed Reaction: Effect of Solvent Viscosity on Kinetic Constants. Biochemistry 2009;48:5510–5517. [PubMed: 19435313]
33. Sievers A, Wolfenden R. The effective molarity of the substrate phosphoryl group in the transition state for yeast OMP decarboxylase. Bioorg Chem 2005;33:45–52. [PubMed: 15668182]
34. Moffatt JG. The synthesis of orotidine 5′-phosphate. J Am Chem Soc 1963;85:1118–1123.
35. Gasteiger E, Gattiker A, Hoogland C, Ivanyi I, Appel RD, Bairoch A. ExPASy: The proteomics server for in-depth protein knowledge and analysis. Nucleic Acids Res 2003;31:3784–3788. [PubMed: 12824418]
36. Gasteiger, E.; Hoogland, C.; Gattiker, A.; Duvaud, S.; Wilkins, MR.; Appel, RD.; Bairoch, A. Proteomics Protocols Handbook. Walker, JM., editor. Humana Press Inc.; Totowa, NJ: 2005. p. 571-607.
37. Herschlag D. The role of induced fit and conformational changes of enzymes in specificity and catalysis. Bioorg Chem 1988;16:62–96.
38. Vielle C, Zeikus GJ. Hyperthermophilic Enzymes: Sources, Uses, and Molecular Mechanisms for Thermostability. Microbiol Mol Biol Rev 2001;65:1–43. [PubMed: 11238984]
39. Wrba A, Schweiger A, Schultes V, Jaenicke R, Zavodszky P. Extremely thermostable D-glyceraldehyde-3-phosphate dehydrogenase from the eubacterium Thermotoga maritima. Biochemistry 1990;29:7584–7592. [PubMed: 2271518]
40. Závodszky P, Kardos J, Svingor, Petsko GA. Adjustment of conformational flexibility is a key event in the thermal adaptation of proteins. Proc Natl Acad Sci U S A 1998;95:7406–7411. [PubMed: 9636162]
41. Tehei M. Neutron Scattering Reveals the Dynamic Basis of Protein Adaptation to Extreme Temperature. J Biol Chem 2005;280:40974–40979. [PubMed: 16203729]
42. Liang Z, Lee T, Resing KA, Ahn NG, Klinman J. Thermal-activated protein mobility and its correlation with catalysis in thermophilic alcohol dehydrogenase. Proc Natl Acad Sci U S A 2004;101:9556–9561. [PubMed: 15210941]
43. Liang ZX, Tsigos I, Bouriotis V, Klinman JP. Impact of Protein Flexibility on Hydride-Transfer Parameters in Thermophilic and Psychrophilic Alcohol Dehydrogenases. J Am Chem Soc 2004;126:9500–9501. [PubMed: 15291528]
44. Brouwer A, Kirsch J. Investigation of diffusion-limited rates of chymotrypsin reactions by viscosity variation. Biochemistry 1982;21:1302–1307. [PubMed: 7074086]
45. Lim W, Raines R, Knowles J. Triosephosphate isomerase catalysis is diffusion controlled. Appendix: Analysis of triose phosphate equilibria in aqueous solution by phosphorus-31 NMR. Biochemistry 1988;27:1165–1167.
46. Chan KK, Wood BM, Fedorov AA, Fedorov EV, Imker HJ, Amyes TL, Richard JP, Almo SC, Gerlt JA. Mechanism of the Orotidine 5′-Monophosphate Decarboxylase-Catalyzed Reaction: Evidence for Substrate Destabilization. Biochemistry 2009;48:5518–5531. [PubMed: 19435314]

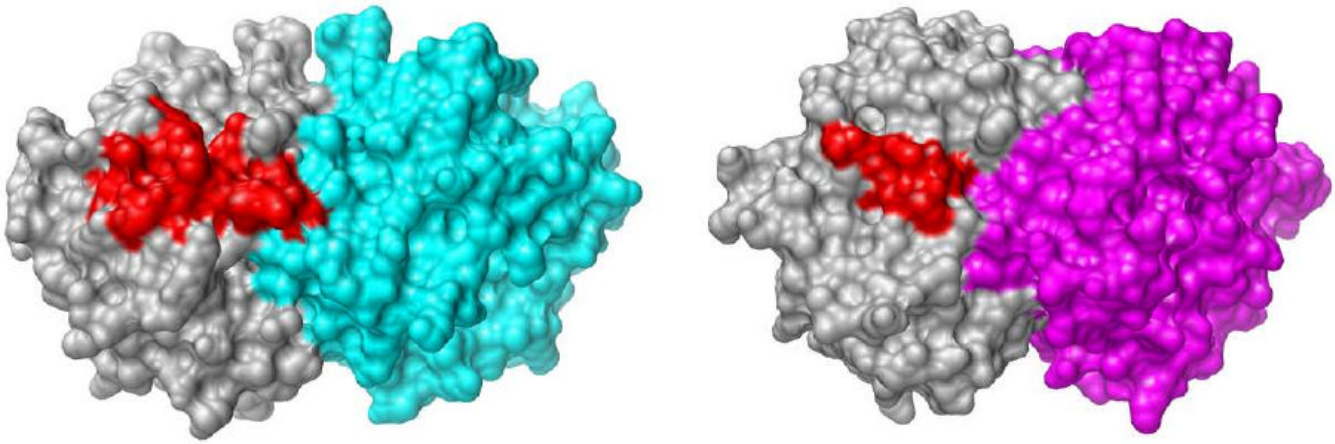

Figure 1.

Comparison of the closed active site loops of the dimeric OMPDCs from *S. cerevisiae* (19 residues, left structure, PDB accession code 3GDL (46)) and *M thermautotrophicus* (9 residues, right structure, PDB accession code 3G1A (46)) liganded with 6-azauridine 5′-monophosphate. The active site loops are shown in red and the remainder of the monomer is shown in grey. The second monomer is shown in cyan (ScOMPDC) or magenta (MtOMPDC). The loop for ScOMPDC extends from Pro-202 to Val-220 and the loop for MtOMPDC extends from Pro-180 to Asp-188. The images were produced using the UCSF Chimera package from the Resource for Biocomputing, Visualization, and Informatics at the University of California, San Francisco (supported by NIH P41 RR-01081).

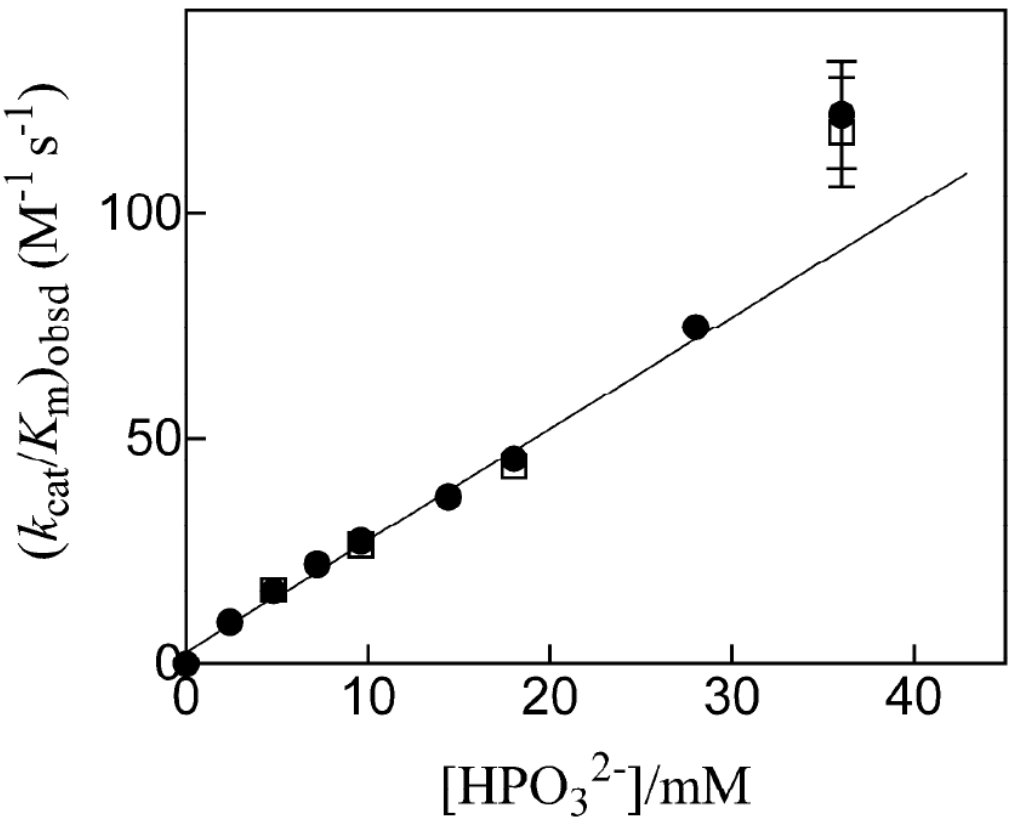

Figure 2.
Dependence of $(k_{cat}/K_m)_{obsd}$ for the decarboxylation of EO catalyzed by MtOMPDC on the concentration of added phosphite dianion at pH 7.0, 25 °C and I = 0.14 (NaCl). The closed and open symbols represent data obtained in two independent experiments that were reproducible to within 5%. The slope of the correlation gives the third-order rate constant $(k_{cat}/K_m)/K_d$ = 2500 M^{-1} s^{-1} for the phosphite-activated reaction. The data at $[HPO_3^{2-}]$ = 36 mM include error bars that indicate the estimated maximum range of experimental error (± 10%) and they were not included in the correlation (see text).

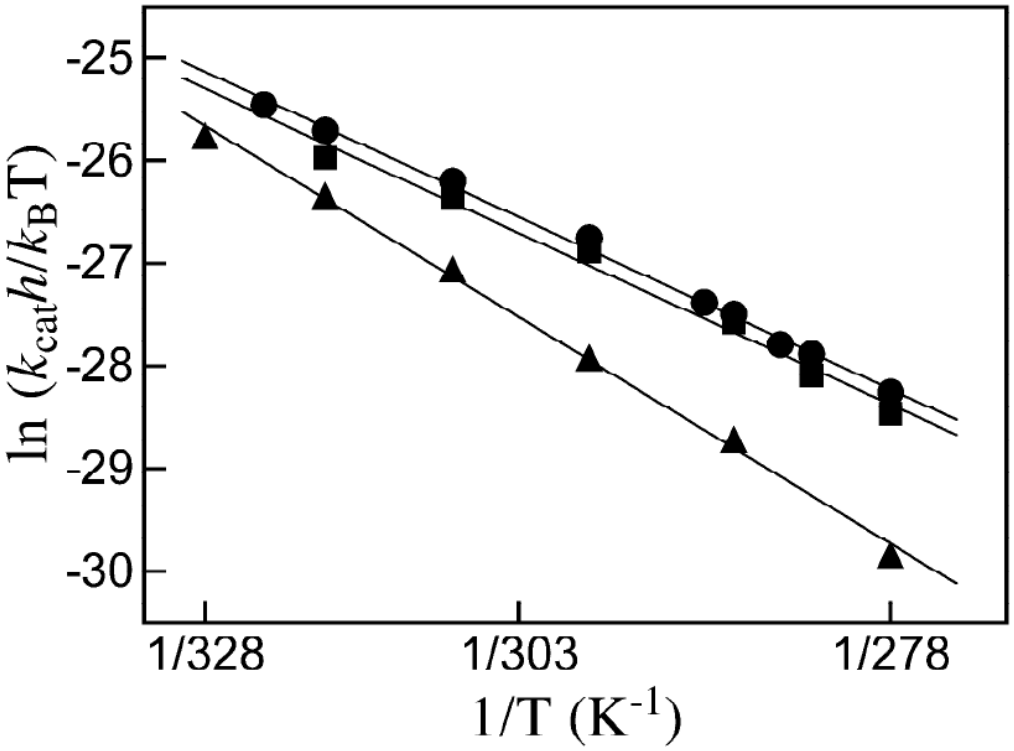

Figure 3.
The temperature dependence of k_{cat} (s^{-1}) for the decarboxylation of saturating OMP catalyzed by OMPDCs from various organisms plotted according to the Eyring equation (eq 3). Key: ●, ScOMPDC; ■, EcOMPDC; ▲, MtOMPDC.

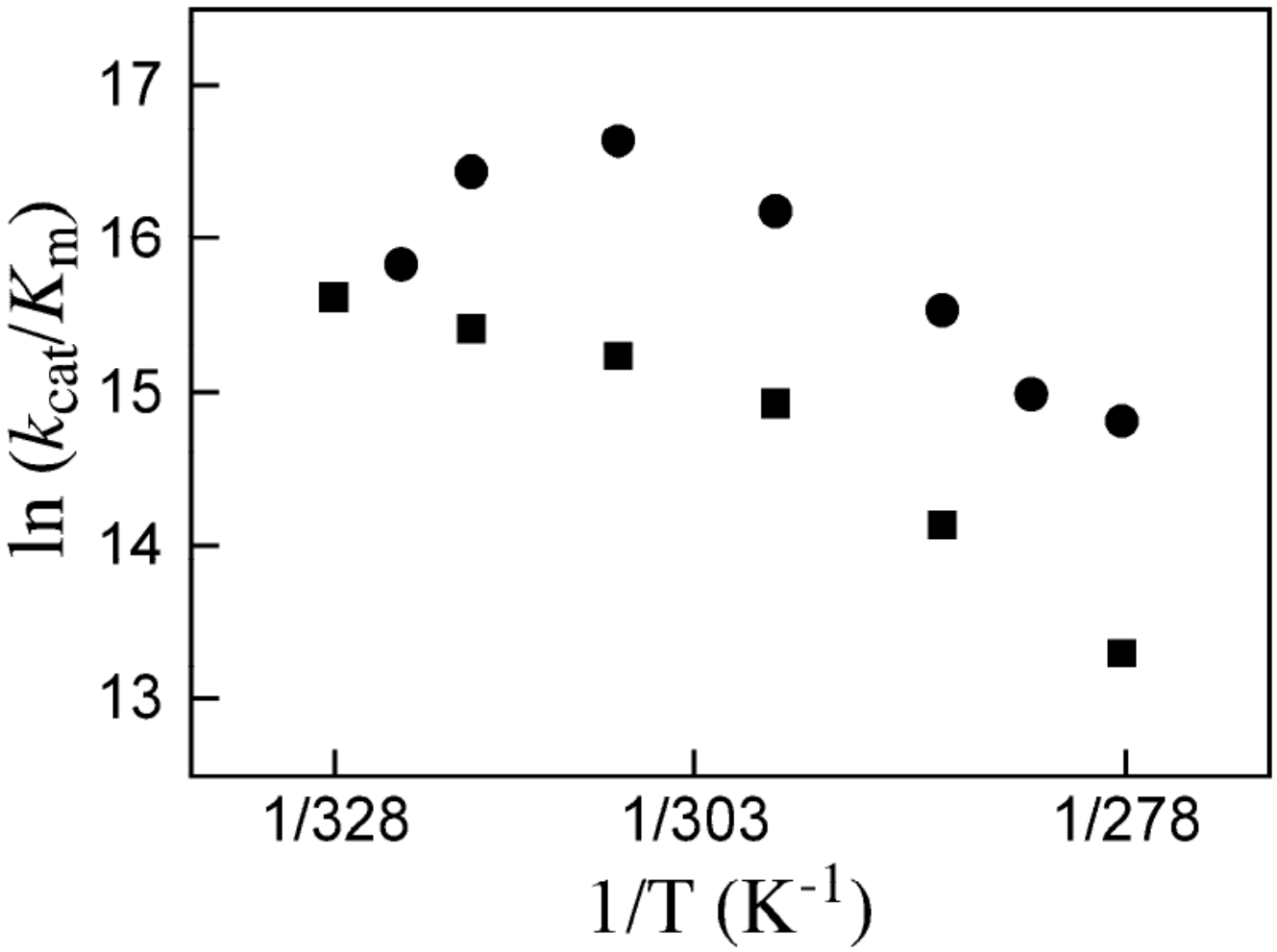

Figure 4.
Correlations of ln (k_{cat}/K_m) with 1/T for the decarboxylation of sub-saturating OMP catalyzed by ScOMPDC (●) and MtOMPDC (■).

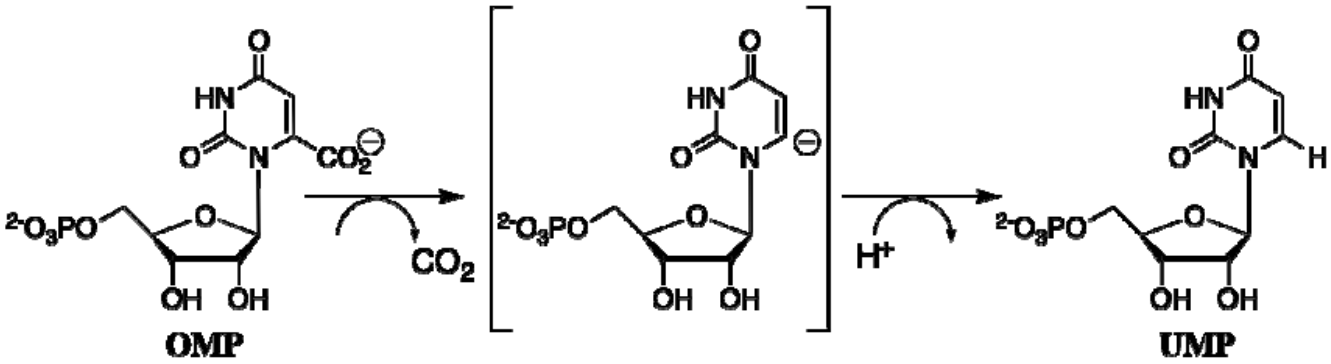

Scheme 1.

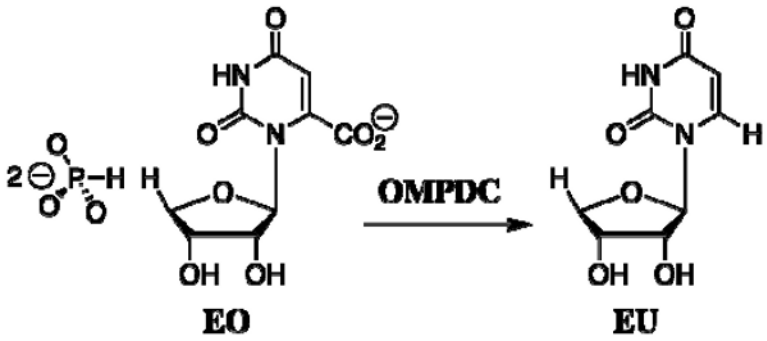

Scheme 2.

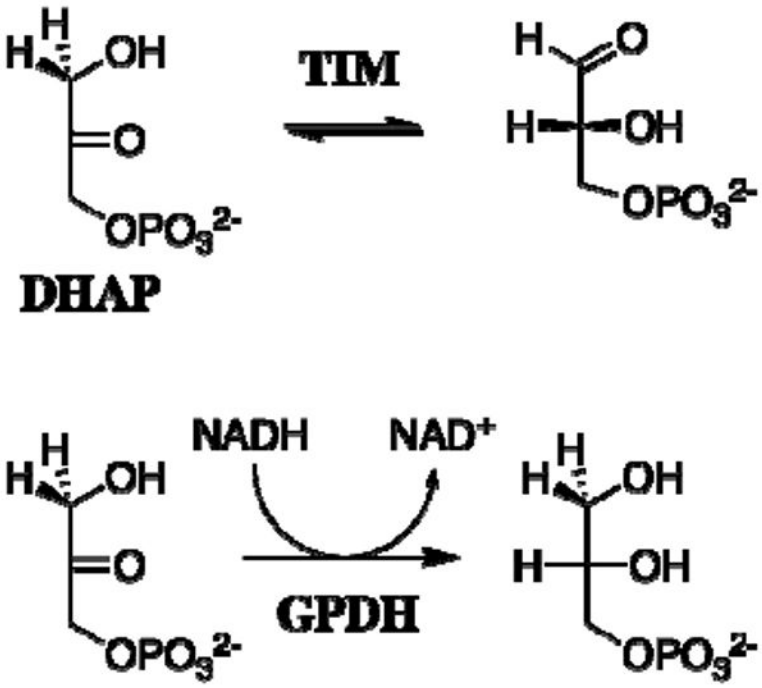

Scheme 3.

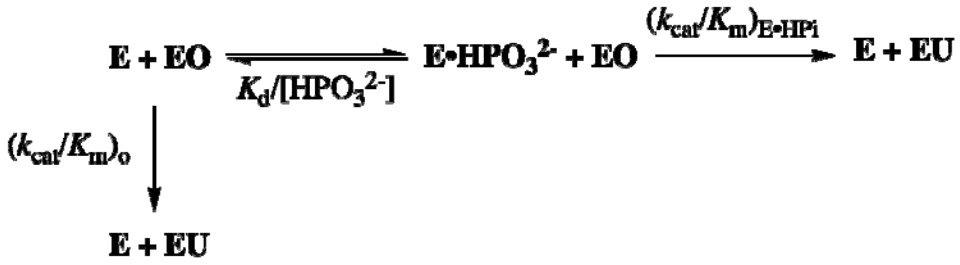

Scheme 4.

Scheme 5.

Table 1

Kinetic parameters and intrinsic phosphate binding energies for decarboxylation of OMP and EO catalyzed by ScOMPDC and MtOMPDC and for the phosphite-activated reactions of EO at pH 7.0 and 25 °C.

	k_{cat}/K_m(M^{-1} s^{-1})		IPBE [b]	$(k_{cat}/K_m)_{E\cdot HPi}/K_d$ [c]	Phosphite Activation [d]
	OMP [a]	EO		$M^{-2}s^{-1}$	
ScOMPDC	1.1×10^7	2.1×10^{-2} [e]	11.9 kcal/mol	11,700 [e]	5.6×10^5 M^{-1}
MtOMPDC	3.1×10^6	8.7×10^{-3}	11.6 kcal/mol	2,500	2.9×10^5 M^{-1}

[a] Data at pH 7.1 from Table 2.

[b] Intrinsic phosphate binding energy calculated from the ratio of the second-order rate constants for the reactions of OMP and EO.

[c] Third-order rate constant for phosphite-activated decarboxylation of EO catalyzed by OMPDC, calculated as the slope of the plot of $(k_{cat}/K_m)_{obsd}$ against $[HPO_3^{2-}]$ at low concentrations of phosphite (Figure 2).

[d] Ratio of the third-order rate constant for the phosphite-activated decarboxylation of EO and the second-order rate constant for the unactivated decarboxylation of EO.

[e] Data at pH 7.1 from Ref. 14.

Table 2

Temperature dependence of the kinetic parameters for decarboxylation of OMP catalyzed by ScOMPDC, MtOMPDC and EcOMPDC at pH 7.1 and I = 0.1 (NaCl).[a]

	ScOMPDC			MtOMPDC			EcOMPDC
Temp °C	k_{cat}[b] s^{-1}	k_{cat}/K_m[c] $M^{-1}\ s^{-1}$	K_m[d] μM	k_{cat}[b] s^{-1}	k_{cat}/K_m[c] $M^{-1}\ s^{-1}$	K_m[d] μM	k_{cat}[b] s^{-1}
5	3.1 ± 0.5	$2.7 \pm 0.2 \times 10^6$	1.1 ± 0.2	0.64 ± 0.03	$6.0 \pm 2.2 \times 10^5$	1.1 ± 0.4	2.5 ± 0.1
10	4.6 ± 0.6	$3.2 \pm 0.2 \times 10^6$	1.4 ± 0.2				3.7 ± 0.1
12	5.1 ± 0.5						
15	6.9 ± 0.9	$5.6 \pm 0.4 \times 10^6$	1.2 ± 0.2	2.0 ± 0.3	$1.4 \pm 0.2 \times 10^6$	1.5 ± 0.3	6.4 ± 0.1
17	7.8 ± 0.8						
25	15 ± 1	$1.1 \pm 0.1 \times 10^7$	1.4 ± 0.2	4.7 ± 0.3	$3.1 \pm 0.3 \times 10^6$	1.5 ± 0.2	13 ± 1
35	27 ± 1	$1.7 \pm 0.4 \times 10^7$	1.6 ± 0.4	11 ± 1	$4.2 \pm 0.9 \times 10^6$	2.8 ± 0.6	23 ± 1
45	45 ± 4	$1.4 \pm 0.2 \times 10^7$	3.3 ± 0.6	24 ± 2	$5.0 \pm 1.3 \times 10^6$	4.8 ± 1.4	35 ± 1
50	59 ± 6	$7.5 \pm 0.3 \times 10^6$	7.9 ± 0.9				
55				44 ± 2	$6.1 \pm 0.9 \times 10^6$	7.3 ± 1.1	

[a] The quoted errors in k_{cat} and k_{cat}/K_m are standard errors that were obtained from multiple experiments to determine these parameters.

[b] Determined from the initial velocity of decarboxylation of OMP when $[OMP]_O \geq 20K_m$. The observed values of k_{cat} were independent of enzyme concentration in the range 11 – 42 nM for ScOMPDC, 76 - 152 nM for MtOMPDC and 30 – 230 nM for EcOMPDC (see text).

[c] Determined from the first-order rate constant for decarboxylation of OMP ($[OMP]_O \leq 40$ μM) when $[OMP]_t = 0.3 - 0.5K_m$ (see text).

[d] Calculated from the values of k_{cat} and k_{cat}/K_m. The standard error was obtained by propagation of the standard errors in k_{cat} and k_{cat}/K_m.

Table 3

Activation parameters for k_{cat} for decarboxylation of OMP catalyzed by OMPDCs from *S. cerevisiae*, *E. Coli* and *M. thermautotrophicus*.[a]

Enzyme	$\Delta H^{\ddagger}$ (kcal mol^{-1}) [b]	$\Delta S^{\ddagger}$ (cal K^{-1} mol^{-1}) [c]
ScOMPDC	11.2	-16
EcOMPDC	11.2	-16
MtOMPDC	14.8	-6.0

[a] For reactions at pH 7.1 and I = 0.1 (NaCl) (data from Table 2). Activation parameters were determined from Eyring plots covering the range 278 – 328 K (5 – 55 °C, Figure 3).

[b] Determined from the slopes of the correlations in Figure 3 according to eq 3.

[c] Determined from the intercepts of the correlations in Figure 3 according to eq 3.